Controlled Drug Delivery

DOI: 10.1002/anie.201406442

Molecularly Precise Dendrimer–Drug Conjugates with Tunable Drug Release for Cancer Therapy**

Zhuxian Zhou, Xinpeng Ma, Caitlin J. Murphy, Erlei Jin, Qihang Sun, Youqing Shen, Edward A. Van Kirk, and William J. Murdoch*

Abstract: *The structural preciseness of dendrimers makes them perfect drug delivery carriers, particularly in the form of dendrimer–drug conjugates. Current dendrimer–drug conjugates are synthesized by anchoring drug and functional moieties onto the dendrimer peripheral surface. However, functional groups exhibiting the same reactivity make it impossible to precisely control the number and the position of the functional groups and drug molecules anchored to the dendrimer surface. This structural heterogeneity causes variable pharmacokinetics, preventing such conjugates to be translational. Furthermore, the highly hydrophobic drug molecules anchored on the dendrimer periphery can interact with blood components and alter the pharmacokinetic behavior. To address these problems, we herein report molecularly precise dendrimer–drug conjugates with drug moieties buried inside the dendrimers. Surprisingly, the drug release rates of these conjugates were tailorable by the dendrimer generation, surface chemistry, and acidity.*

Dendrimers are monodisperse three-dimensional macromolecules and have been applauded as platforms for drug[1,2] and gene delivery[3] owing to their unique highly branched and precise molecular structures, ample surface groups for functionalizations, and internal cavities for host–guest encapsulations[4,5] as well as low intrinsic viscosity facilitating transport in blood.[6] Those characteristics are particularly epitomized in dendrimer–drug conjugates, which are generally synthesized by anchoring drug and functional moieties onto the peripheral surface.[4c,7] This approach is advantageous with regard to the easy synthesis; however, it sacrifices the unique feature of dendrimers, that is, the preciseness of their molecular structure, because the high amount of functional groups with the same reactivity make it impossible to precisely control the number and the position of the functional groups and drugs anchored to the dendrimer surface.[8] Such structural heterogeneity causes variable pharmacokinetics and is the major hurdle for dendrimer–drug conjugates to be translational.[9] Additionally, the drug molecules, usually highly hydrophobic, anchored on the dendrimer periphery can interact with blood components, thereby altering the pharmacokinetics.[10] Herein, we report molecularly precise dendrimer–drug conjugates with drug moieties buried inside the dendrimer structure. Surprisingly, the drug release rates of these conjugates were tunable by the dendrimer generation, surface chemistry, and acidity (Figure 1 A).

The conjugates were synthesized using camptothecine (CPT) as the core-forming compound. CPT is a potent topoisomerase inhibitor showing strong antitumor activity,[11] but it is too hydrophobic to be administered and has shown severe side effects in clinical use.[12] CPT was first reacted with *N*-Boc-glycine followed by deprotection to prepare camptothecin-20(*S*)-glycinate ester (CPT-NH_2). The ester was reacted with *N*-Boc-protected lysine followed by deprotection. Repeating this step produced the CPT-cored polylysine dendrimers of different generations (CPT-G*x*), e.g., the fifth generation PLL dendrimer conjugated with CPT, CPT-G5 (Figure 1 B and Figure S1 in the Supporting Information). As characterized by MALDI-TOF MS (Figure 1 C) and other methods (NMR spectroscopy, HPLC, and UV/Vis spectroscopy, Figures S2–S4), all CPT-G*x* had precise molecular structures. They were all monodisperse and the molecular weights were consistent with the theoretical values (Figure 1 C and Figure S3 for HPLC traces). The CPT contents of the conjugates were determined by ^{1}H NMR spectroscopy and were also consistent with the molecular structures (Table S1 and Figure S2). Each conjugate contained one CPT molecule buried in its core and thus the CPT content was fixed. The low generation conjugates had high CPT contents, but CPT-G5 still contains 8.0 wt% CPT, higher than most dendrimer–drug conjugates.

The drug release of dendrimer–drug conjugates is generally realized by the cleavage of drug linkages, which can be enzyme-labile peptides,[13] pH- or external-stimuli-labile bonds,[1a,9c,15] and disulfide bonds.[1b,14] CPT-G*x* showed a very interesting generation-dependent CPT release (Figure 2 A and Figure S5). The fastest CPT release was observed with CPT-G1, whereas the slowest release was found for CPT-

[*] Prof. Y. Shen
Center for Bionanoengineering and State Key Laboratory of Chemical Engineering
Department of Chemical and Biological Engineering
Zhejiang University, Hangzhou, 310027 (China)
E-mail: shenyq@zju.edu.cn
Homepage: http://che.zju.edu.cn/others/bionano/English
Dr. Z. Zhou, Dr. X. Ma, Dr. E. Jin, Dr. Q. Sun
Department of Chemical and Petroleum Engineering
University of Wyoming, Laramie, 82071 (USA)
Dr. C. J. Murphy, E. A. Van Kirk, Prof. W. J. Murdoch
Department of Animal Science
University of Wyoming, Laramie, 82071 (USA)

[**] This study was funded by the National Natural Science Foundation Key Program (21090352 and 51390481), the National Basic Research Program (2014CB931900), the National Fund for Distinguished Young Scholars (50888001), the Doctoral Fund of Ministry of Education of China (20110101130007), and the US Department of Defence (BC090502).

Supporting information for this article is available on the WWW under http://dx.doi.org/10.1002/anie.201406442.

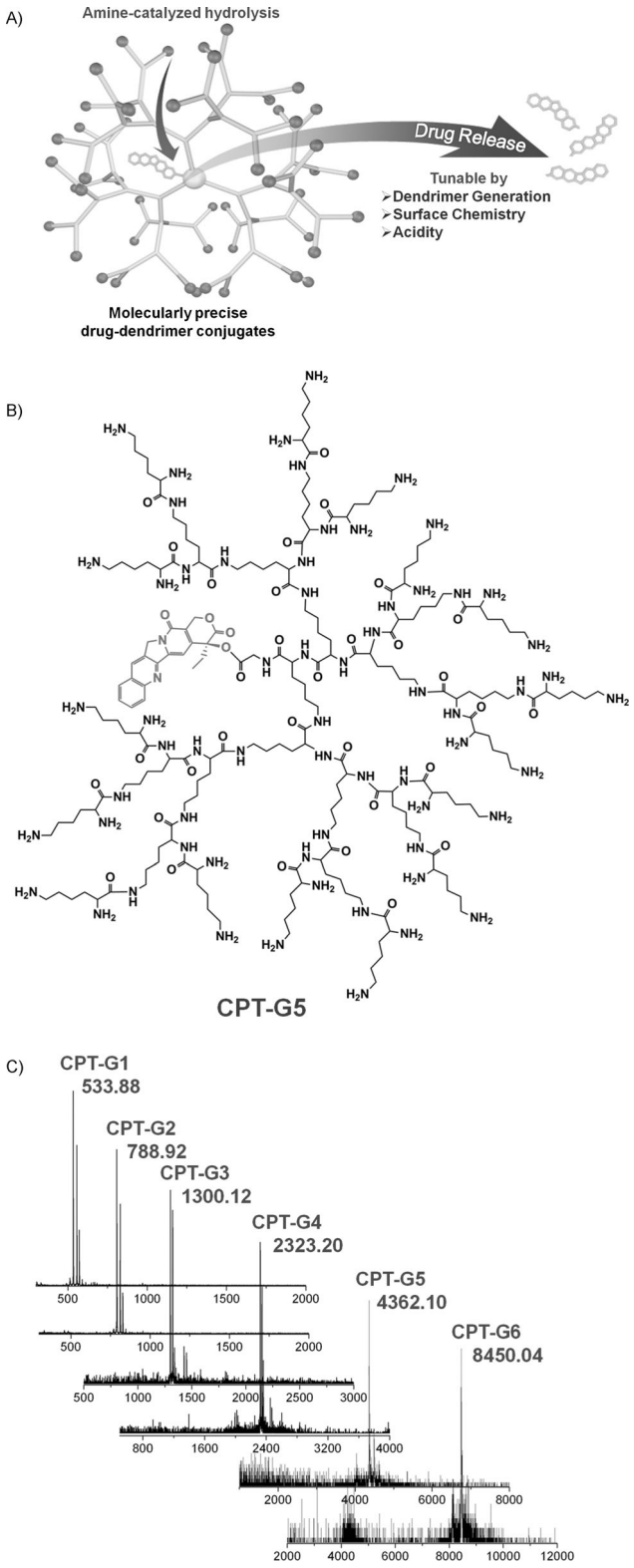

Figure 1. A) Molecularly precise camptothecine–polylysine dendrimer (PLL) conjugate and its drug release tunable by dendrimer generation, surface chemistry, or acidity. B) The structure of CPT-5th generation PLL (CPT-G5). C) The MALDI-TOF MS spectra of the CPT conjugates with different generation PLLs (CPT-G*x*).

G2 and then increased with increasing dendrimer generation. The time needed to release 50 % of the CPT (t_{50}) was only 0.42 h for CPT-G1 but 21.3 h for CPT-G2, and gradually decreased to 5.3 h for CPT-G6. Due to the protonation of the amine, the CPT-release was slower at acidic pH (Figure 2 A). These results indicate that CPT release from CPT-G*x* is an amine-promoted hydrolysis of the CPT ester. The high amount of amine groups at high dendrimer generations may be responsible for the fast CPT release. In aqueous solutions, the terminal primary amines underwent nucleophilic attack of the lactone carbonyl electrophile,[16] producing intermediates eventually releasing active CPT (Figure S5). CPT-G1 had the fastest CPT release rate, which is probably due to the favored amine-promoted hydrolysis by intramolecular six-membered-ring formation.[16]

Since the CPT release from CPT-G*x* was catalyzed by peripheral amine groups, we proposed that an amidation of the peripheral amines might further tune the CPT release rate. Using CPT-G5 as an example, its 32 primary amines were reacted with controlled amounts of *O*-[2-(2-methoxyethoxy)-ethyl]glycolic acid pentafluorophenol ester [$(EG)_3$-COO-PFP] to produce conjugates with amidation degrees of 20 %, 40 %, 60 %, 80 %, and 100 % (CPT-G5OEG), respectively, as determined by ^{1}H NMR spectra and HPLC (Figure S6). The t_{50} values accordingly increased from 8.6 h to 14.9, 28.1, 32.4, 49.6, and 157.2 h, respectively (Figure 2 B). Thus, the CPT release of CPT-G5 was indeed tunable by the amidation of surface amine groups.

For cancer drug delivery it is desirable to avoid drug release at physiological pH, but achieve a quick release in the acidic tumor extracellular fluid (pH ≈ 6–7[17]) or intracellular lysosomes (pH ≈ 4–5[17]).[18] Some β-carboxylic amides are stable at neutral or basic pH but quickly hydrolyze to regenerate the original amines.[1b,19] Thus, we further propose that the amidation of the CPT-G*x* amines to such β-carboxylic amides would inhibit the CPT release; however, in an acidic environment would hydrolyze the amides and regenerate the amine to promote CPT release. Along this line, CPT-G5 was reacted with succinic anhydride (CPT-G5SA), 1,2-dicarboxylic-cyclohexene anhydride (CPT-G5DCA), or 2,3-dimethylmaleic anhydride (CPT-G5DM) (Figure 2 C and Table S1). According to the ^{1}H NMR spectrum and HPLC data, the amidation of CPT-G5SA of CPT-G5DCA and CPT-G5DM were 100 %, 85 %, and 78 %, respectively (Figures S6 and S7). Measurements of the zeta potential showed that in contrast to the positively charged CPT-G5 (9.42 mV), the resulting amidated conjugates, CPT-G5DM, CPT-G5DCA, and CPT-G5SA were all negatively charged, −12.9 mV, −17.3 mV, and −22.3 mV, respectively. The time-dependent zeta potentials of CPT-G5SA, CPT-G5DM, and CPT-G5DCA are shown in Figure S8. The amide groups of CPT-G5OEG cannot hydrolyze and this compound was used as a control. The zeta potential of CPT-G5SA did not significantly change with time at both pH 7.4 and 6.0 because the succinic amide of primary amines is hardly hydrolysable under weakly acidic conditions.[1b] At pH 7.4, CPT-G5DM gradually became positively charged within 2.5 h, whereas CPT-G5DCA remained negatively charged even after 24 h. At pH 6.0, CPT-G5DM and CPT-G5DCA became positively charged within 0.25 h and

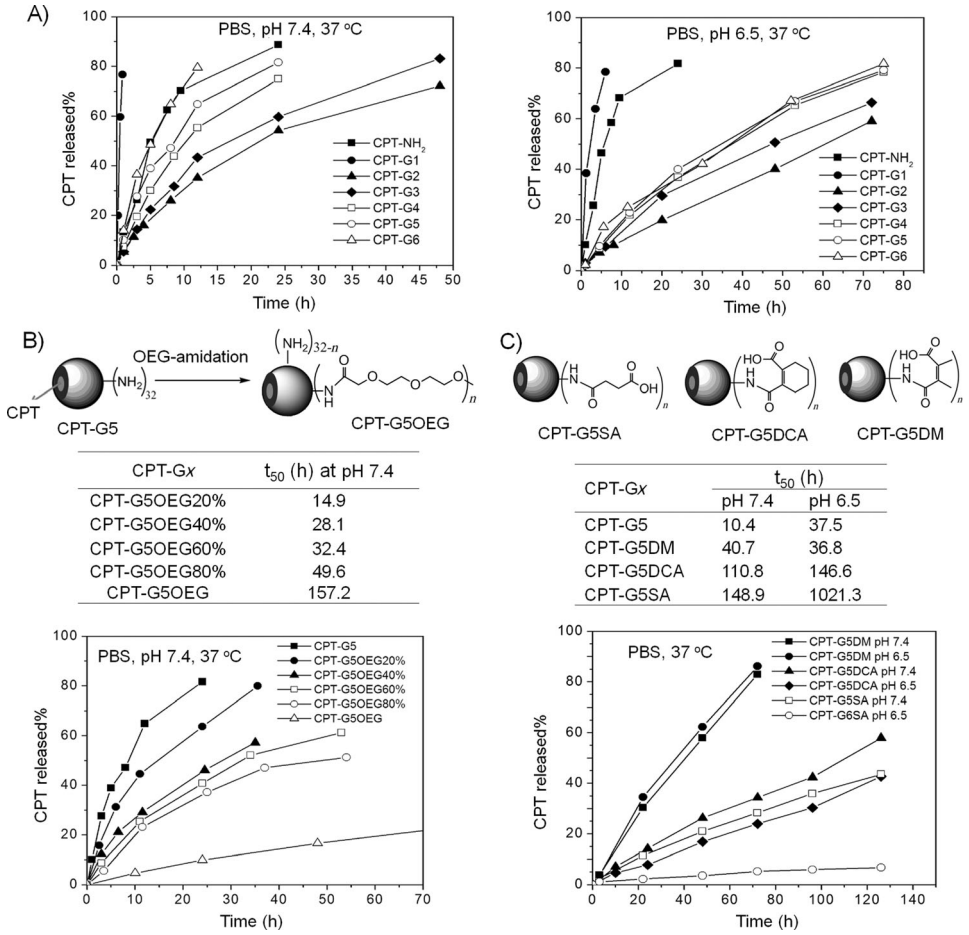

CPT-G*x*	t_{50} (h) at pH 7.4
CPT-G5OEG20%	14.9
CPT-G5OEG40%	28.1
CPT-G5OEG60%	32.4
CPT-G5OEG80%	49.6
CPT-G5OEG	157.2

CPT-G*x*	t_{50} (h)	
	pH 7.4	pH 6.5
CPT-G5	10.4	37.5
CPT-G5DM	40.7	36.8
CPT-G5DCA	110.8	146.6
CPT-G5SA	148.9	1021.3

Figure 2. A) The CPT release kinetics of CPT-G*x* with different generation. B) Amidation of CPT-G5 with *O*-[2-(2-methoxyethoxy)ethyl]glycolic acid (CPT-G5OEG) at various amidation degrees. C) Amidation of CPT-G5 with succinic anhydride (CPT-G5SA), 1,2-dicarboxylic-cyclohexene anhydride (CPT-G5DCA), and 2,3-dimethylmaleic anhydride (CPT-G5DM).

4.3 h, respectively, indicating the hydrolysis of the amides and the regeneration of the primary amine.[19a] This also indicates that the amide resulting from 2,3-dimethylmaleic anhydride (DM) is much more acid-labile than the amide resulting from 1,2-dicarboxylic-cyclohexene anhydride (DCA). Accordingly, at pH 7.4 the CPT-release from CPT-G5SA, CPT-G5DCA, and CPT-G5DM was significantly decreased compared with that from CPT-G5. At pH 6.5, the acid-labile CPT-G5DM quickly hydrolyzed and recovered the amines, and thus it had a CPT release rate similar to that of CPT-G5 at this pH ($t_{50} \approx 37$ h), whereas the slowly hydrolysable CPT-G5DCA released CPT slowly ($t_{50} \approx 146$ h) and CPT-G5SA hardly released any CPT at this acidic pH. Thus, the amidation of the CPT-G5 peripheral amines could tailor the CPT release rate by controlling the acid lability of the β-carboxylic amides. Another advantage of these amidated conjugates is their neutral or negatively charged surface, which reduces the plasma protein adsorption and lowers the nonspecific cellular uptake for in vivo applications; however, as soon as the nanocarriers reach, e.g., the acidic tumor extracellular fluid, the amines would be recovered and accelerate the CPT release and cellular uptake.

The cellular uptake of CPT-G5 and its amidated products were measured by flow cytometry after labeling with a fluorescent dye Cy5 (Figure 3 A). At pH 7.4, CPT-G5/Cy5 showed a faster cellular uptake than the amidated compounds, which is due to its positive charge-induced electrostatic adsorption.[19a] For CPT-G5DM/Cy5 pH-dependent cellular uptake rates were observed. The cells cultured with CPT-G5DM/Cy5 at pH 6.5 had a fluorescent intensity that was 3.6 times higher than that of the cells cultured at pH 7.4. In contrast, the cellular uptake of CPT-G5SA/Cy5 or CPT-G5OEG/Cy5 at pH 7.4 and 6.5 were very similar; suggesting that the amidation of CPT-G5 to CPT-G5DM reduced the nonspecific cellular uptake at neutral pH but regained the high cellular uptake in acidic tumor fluid. The cellular uptake of the different conjugates was further investigated by confocal microscopy (Figure 3 B). CPT-G5/Cy5 at both pH values and CPT-G5DM/Cy5 at pH 6.5 were mainly present in the cells and not in the lysosomes/endosomes, whereas much less CPT-G5SA/Cy5 and CPT-G5OEG/Cy5 was found in the cells and appeared as yellow spots in the overlay images of the fluorescence of Cy5 and lysotracker, indicating that they were trapped in lysosomes/endosomes. Protonation and the resulting positive charges of CPT-G5/Cy5 and CPT-G5DM/Cy5 enabled them to escape from the lysosomes/endosomes through the "proton-sponge" effect,[1b] but the noncharge-reversal CPT-G5SA/Cy5 and CPT-G5OEG/Cy5 could not

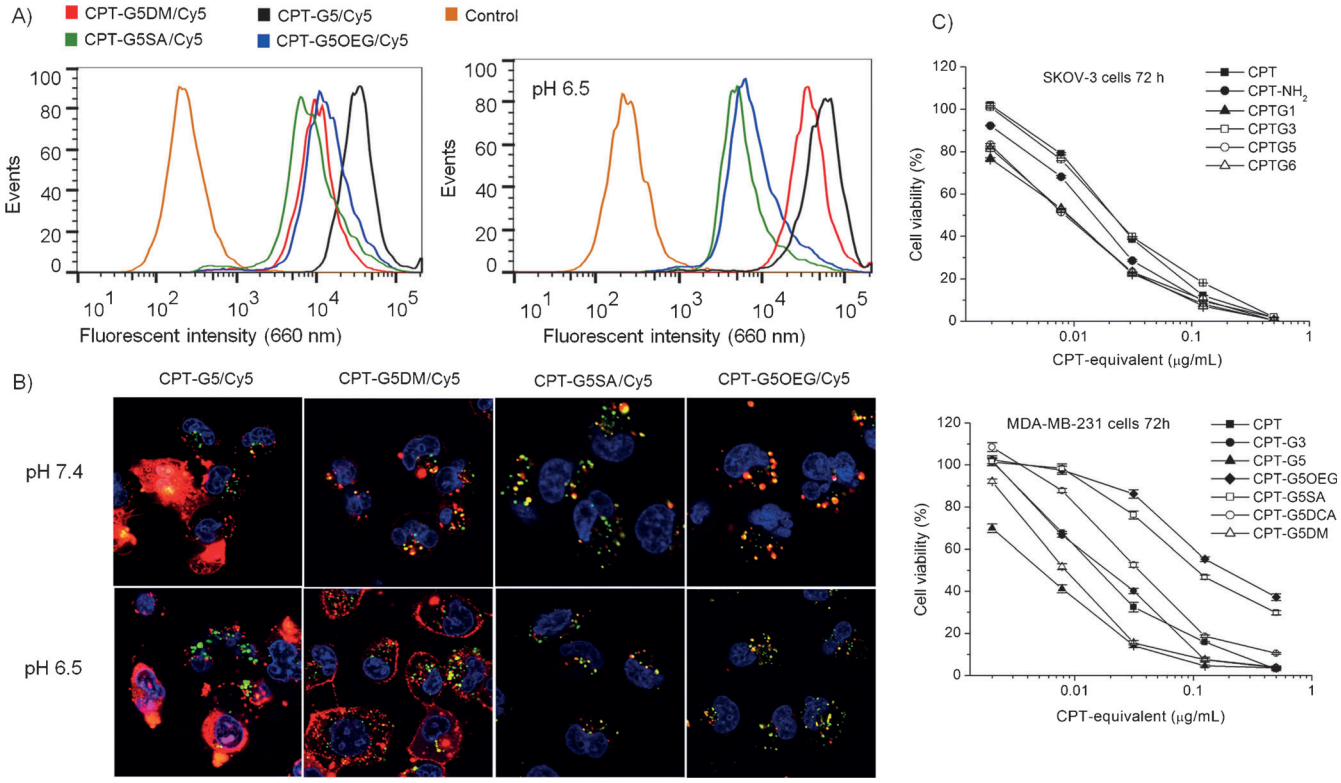

Figure 3. Cellular uptake of CPT-G5 and its amidated products labeled with a fluorescent dye Cy5 (CPT-G5/Cy5, CPT-G5DM/Cy5, CPT-G5SA/Cy5, and CPT-G5OEG/Cy5) measured A) by flow cytometry and B) investigated by confocal microscopy (dendrimer–Cy5: red; LysoTracker: green; nuclear dye Hoechst 33342: blue). The cells were cultured with CPT-G5amide/Cy5 (Cy5 equivalent 1 μM) for 3 h at pH 7.4 or 6.5. C) The cytotoxicity of CPT and the conjugates against SKOV-3 and MDA-MB-231 cells cultured for 72 h was estimated by the MTT assay. Data represent the mean values ± standard deviation, $n = 5$.

escape due to their negative charges and inability to induce the "proton-sponge" effect.

The cytotoxicity of the conjugates against SKOV-3 ovarian cancer cells and MDA-MB-231 breast cancer cells were compared using the MTT assay (Figure 3C and Figure S9). To both of the cell lines, CPT-G*x* showed a generation-dependent cytotoxicity corresponding to the CPT release rate, which is consistent with the previous finding that a faster intracellular release from nanocarriers leads to a higher cytotoxicity.[20,21] The IC_{50} values of CPT-G*x* to SKOV-3 or MDA-MB-231 cancer cells were as low as 8.5 and 5.1 ng mL^{-1}, in comparison to those of CPT, which are 21 and 16 ng mL^{-1}, respectively. Acid-labile CPT-G5DM showed cytotoxicity very comparable to that of CPT-G5, but the slow CPT-releasing CPT-G5OEG and CPT-G5SA were much less cytotoxic (Figure 3C).

The positively charged CPT-G*x* may have a rapid clearance from the blood circulation[22] and thus may not be suitable for intravenous tumor treatments, but could be useful for local cancer treatment.[23] Advanced ovarian cancer is known to easily spread to intraperitoneal (ip) cavities and ip treatment is recommended as a preferred method. Thus, the ip treatment of ovarian tumors was used as a model to evaluate the in vivo antitumor activity of CPT-G5 (Figure 4). Athymic mice bearing ip SKOV-3 ovarian tumors were treated by ip injection of CPT-G5 or CPT at a dose of 1 mg CPT equivalent per kg (Figure 4A). CPT-G5 was found to significantly suppress tumor growth compared to both PBS ($P = 0.00005$ by weight, $P = 0.00034$ by number) and CPT ($P = 0.00214$ by weight, $P = 0.0237$ by number) (Figure 4B–D). The tumors in the mice treated with CPT-G5 had fewer blood vessels (indicated by "*" in Figure 4E) and more pyknotic cells, which had highly condensed pyknotic nuclei (indicated by arrows in Figure 4E) and are considered as apoptotic or dead cells.[20] Moreover, an in situ TUNEL assay showed the highest level of cell apoptosis in the tumors treated with CPT-G5 (Figure 4F), indicating that the enhanced tumor growth inhibition activity of CPT-G5 resulted from its increased proapoptotic effect. This improved efficacy of CPT-G5 may be a combined result of the stabilized active lactone form of CPT buried in the core of the dendrimer, the fast cellular uptake, and the fast release. In addition, no significant weight change of the mice was observed during the 28 day treatment, indicating the low toxicity of ip-injected CPT-G5 (Figure S10).

The amidated CPT-G5 conjugates were neutral or negatively charged and thus may be useful for intravenous cancer treatments. Thus, their anticancer activities were evaluated by iv treatment of athymic mice bearing a subcutaneous (sc) MDA-MB-231-GFP breast tumor (Figure 5). Both free CPT and CPT-G5OEG slowed the tumor growth, but could not stop it even after seven injections. However, one injection of CPT-G5DM or two injections of CPT-G5 stopped the tumor growth and further treatments nearly eradicated the tumors

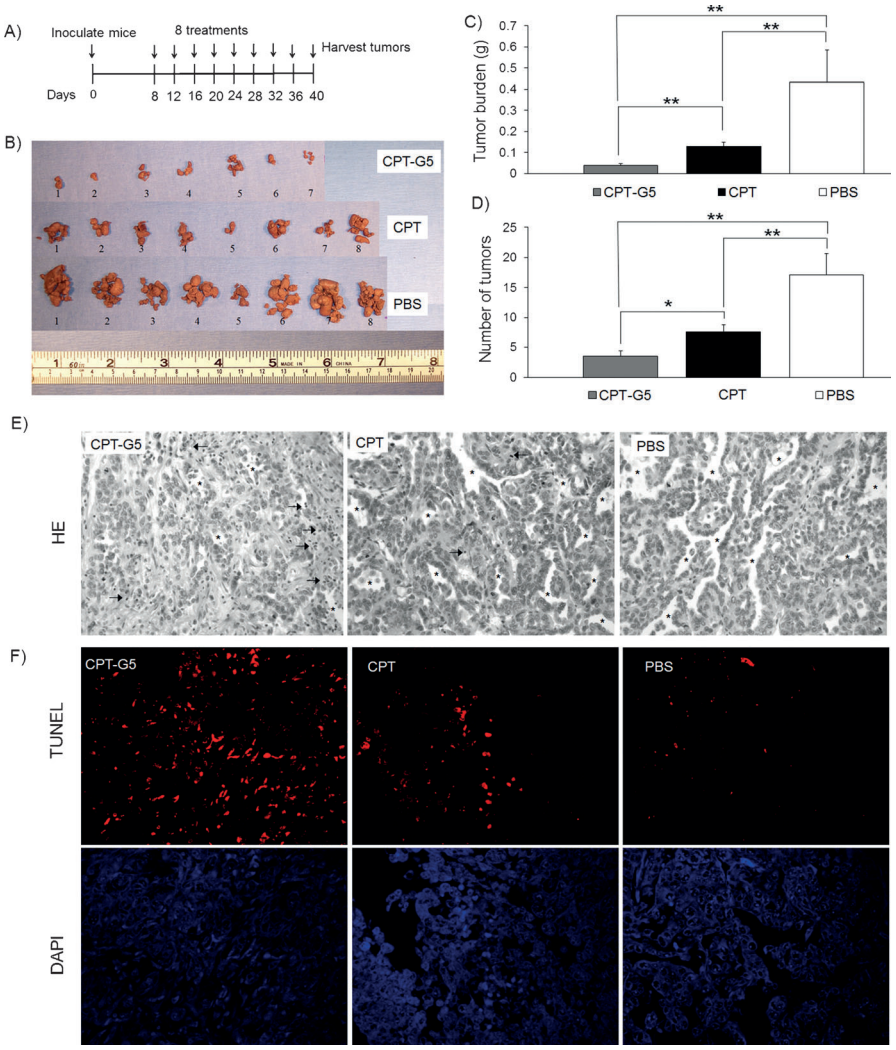

Figure 4. A) The experimental timeline and dosing schedule following the ip tumor inoculation. Athymic mice were ip-injected with SKOV-3 ovarian cancer cells (10^7). The treatment was achieved by ip injection of CPT-G5 or CPT (1 mg CPT equivalents per kg) or PBS ($n = 10$). B) The image of the tumors harvested from the mice and C) the average tumor weight or D) number per mouse in each group after eight treatments. (*) $P < 0.05$, (**) $P < 0.01$. E) Representative histological sections of the tumors stained with hematoxylin and eosin; blood vessels are marked by *; some typical pyknotic cells (highly condensed pyknotic nuclei) are indicated by arrows. F) The TUNEL labeling for apoptosis in the tumor tissues was visualized by BrdUTP incorporation and detected using red fluorescence labeled anti-BrdU monoclonal antibody (red) and DAPI for the nuclei (blue).

(Figure 5B,C and Figure S11). CPT-G5DM and CPT-G5 were found to significantly suppress tumor growth compared to both PBS and CPT ($P < 0.01$) (Figure S11). TUNEL analysis showed that the tumor inhibition activities of the conjugates were directly correlated to their apoptosis-inducing activities. Significantly more apoptotic cells were found in the tumors treated with CPT-G5 or CPT-G5DM than in the other groups (Figure 5F). The blood clearance study (Figure 5D) revealed that CPT was quickly removed from the blood, accounting for its low activity. CPT-G5DM and CPT-G5OEG showed longer blood retention times than CPT-G5, and thus it can be concluded that the amidation of CPT-G5 indeed slowed its clearance from the blood. The similar blood circulation time but lower therapeutic efficacy of CPT-G5OEG compared with CPT-G5DM indicates that the slow drug release from the carrier (Figure 2) deteriorates the drug activity. In contrast, the high efficacy of CPT-G5DM may result from its charge-reversal capability, which enabled the conjugate to retain in the blood for a longer time, thereby enabling accumulation in the tumor by the enhanced permeation and retention effect.[24] The positive charges are regenerated quickly once the conjugate is in the tumor or the cell lysosomes, leading to a fast cellular uptake and fast drug release.[19,25] Very surprisingly, CPT-G5 also had strong anticancer activity even though its circulation time was very short. However, it caused mice to lose about 10% body weight within the first week of treatment and the mice could not recover during the whole treatment period (Figure S12). Thus, CPT-G5 may be suitable only for ip treatment as discussed above, but not for iv treatment. In contrast, the body weights of mice treated with CPT-G5DM slightly decreased in the first week, but quickly recovered thereafter. There was no significant differ-

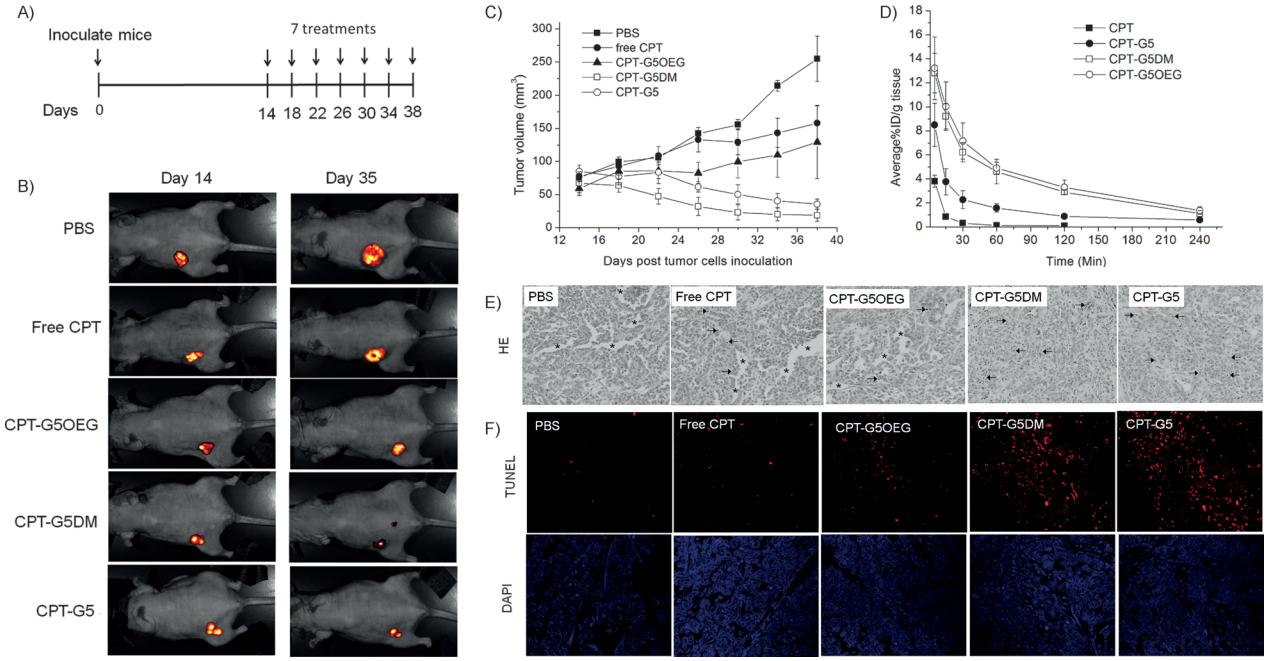

Figure 5. A) The treatment timeline and dosing schedule after the subcutaneous tumor inoculation in nude mice of MDA-MB-231-GFP breast cancer cells (10^6). The treatment was achieved by tail vein injection of CPT or the conjugates at 2.5 mg CPT equivalents per kg (each group $n=4$). B) Representative in vivo Maestro fluorescent imaging of MD-MB-231-GFP tumors in nude mice before (day 14) and after six treatments (day 35). C) The average tumor weight per mouse as a function of time of each group. D) The blood clearance profiles after a single tail vein injection of 2.5 mg CPT equivalents per kg. E) Representative histological sections of the tumors stained with hematoxylin and eosin; blood vessels are marked by *; some typical pyknotic cells (highly condensed pyknotic nuclei) are indicated by arrows. F) The TUNEL labeling for apoptosis in the tumor tissues was visualized by BrdUTP incorporation and detected using red fluorescence labeled anti-BrdU monoclonal antibody (red) and DAPI for nuclei (blue).

ence in the body weight between the groups treated with CPT-G5DM and PBS at the later period, suggesting that CPT-G5DM had a low systemic toxicity.

In summary, we synthesized camptothecin-cored poly(L-lysine) dendrimers as macromolecular prodrugs for cancer therapy. These CPT–dendrimer conjugates exhibit precise molecular structures and fixed drug contents. The drug release rates are tunable by the dendrimer's generation, the peripheral amine groups, the amidation of these amines, and the pH. CPT-G5 had a much improved antitumor efficacy in ip tumor treatment and its amidated analogue showed a stronger antitumor efficacy compared with free CPT in the systemic treatment of sc tumors with a greatly decreased toxicity.

Received: June 21, 2014
Revised: July 29, 2014
Published online: August 25, 2014

Keywords: camptothecin · drug delivery · dendrimers · prodrugs · drug release

[1] a) C. C. Lee, E. R. Gillies, M. E. Fox, S. J. Guillaudeu, J. M. J. Frechet, E. E. Dy, F. C. Szoka, *Proc. Natl. Acad. Sci. USA* **2006**, *103*, 16649 – 16654; b) Y. Shen, Z. Zhou, M. Sui, J. Tang, P. Xu, E. A. Van Kirk, W. J. Murdoch, M. Fan, M. Radosz, *Nanomedicine* **2010**, *5*, 1205 – 1217; c) J. Lim, E. E. Simanek, *Adv. Drug Delivery Rev.* **2012**, *64*, 826 – 835; d) D. Shcharbin, A. Shakhbazau, M. Bryszewska, *Expert Opin. Drug Delivery* **2013**, *10*, 1687 – 1698.

[2] a) M.-H. Park, S. S. Agasti, B. Creran, C. Kim, V. M. Rotello, *Adv. Mater.* **2011**, *23*, 2839 – 2842; b) K. T. Al-Jamal, W. T. Al-Jamal, J. T. W. Wang, N. Rubio, J. Buddle, D. Gathercole, M. Zloh, K. Kostarelos, *ACS Nano* **2013**, *7*, 1905 – 1917; c) G. M. Ryan, L. M. Kaminskas, J. B. Bulitta, M. P. McIntosh, D. J. Owen, C. J. H. Porter, *J. Controlled Release* **2013**, *172*, 128 – 136.

[3] a) X. Xu, H. Yuan, J. Chang, B. He, Z. Gu, *Angew. Chem. Int. Ed.* **2012**, *51*, 3130 – 3133; *Angew. Chem.* **2012**, *124*, 3184 – 3187; b) T. Yu, X. Liu, A. L. Bolcato-Bellemin, Y. Wang, C. Liu, P. Erbacher, F. Qu, P. Rocchi, J. P. Behr, L. Peng, *Angew. Chem. Int. Ed.* **2012**, *51*, 8478 – 8484; *Angew. Chem.* **2012**, *124*, 8606 – 8612; c) Ref. [1d].

[4] a) M. A. Mintzer, M. W. Grinstaff, *Chem. Soc. Rev.* **2011**, *40*, 173 – 190; b) J. B. Wolinsky, M. W. Grinstaff, *Adv. Drug Delivery Rev.* **2008**, *60*, 1037 – 1055; c) S. H. Medina, M. E. H. El-Sayed, *Chem. Rev.* **2009**, *109*, 3141 – 3157.

[5] a) L. M. Kaminskas, V. M. McLeod, C. J. H. Porter, B. J. Boyd, *Mol. Pharm.* **2012**, *9*, 355 – 373; b) T. Zhou, P. Chen, L. Niu, J. Jin, D. Liang, Z. Li, Z. Yang, D. Liu, *Angew. Chem. Int. Ed.* **2012**, *51*, 11271 – 11274; *Angew. Chem.* **2012**, *124*, 11433 – 11436; c) X. Ma, J. Tang, Y. Shen, M. Fan, H. Tang, m. Radosz, *J. Am. Chem. Soc.* **2009**, *131*, 14795 – 14803; d) X. Ma, Z. Zhou, E. Jin, Q. Sun, B. Zhang, J. Tang, Y. Shen, *Macromolecules* **2013**, *46*, 37 – 42.

[6] M. T. Morgan, Y. Nakanishi, D. J. Kroll, A. P. Griset, M. A. Carnahan, M. Wathier, N. H. Oberlies, G. Manikumar, M. C. Wani, M. W. Grinstaff, *Cancer Res.* **2006**, *66*, 11913 – 11921.

[7] S. Biswas, N. S. Dodwadkar, A. Piroyan, V. P. Torchilin, *Biomaterials* **2012**, *33*, 4773 – 4782.

[8] a) D. G. Mullen, E. L. Borgmeier, M. Fang, D. Q. McNerny, A. Desai, J. R. Baker, B. G. Orr, M. M. B. Holl, *Macromolecules*

2010, *43*, 6577 – 6587; b) I. F. Hakem, M. R. Bockstaller, A. M. Leech, J. D. Johnson, S. J. Donahue, J. P. Walker, *J. Am. Chem. Soc.* **2010**, *132*, 16593 – 16598.

[9] a) D. G. Mullen, M. M. B. Holl, *Acc. Chem. Res.* **2011**, *44*, 1135 – 1145; b) L. M. Kaminskas, B. J. Boyd, C. J. H. Porter, *Nanomedicine* **2011**, *6*, 1063 – 1084; c) S. Zhu, M. Hong, G. Tang, L. Qian, J. Lin, Y. Jiang, Y. Pei, *Biomaterials* **2010**, *31*, 1360 – 1371.

[10] a) C. A. Boswell, E. E. Mundo, C. Zhang, D. Bumbaca, N. R. Valle, K. R. Kozak, A. Fourie, J. Chuh, N. Koppada, O. Saad, H. Gill, B. Q. Shen, B. Rubinfeld, J. Tibbitts, S. Kaur, F. P. Theil, P. J. Fielder, L. A. Khawli, K. Lin, *Bioconjugate Chem.* **2011**, *22*, 1994 – 2004; b) B. S. Lee, K. Park, S. Park, G. C. Kim, H. J. Kim, S. Lee, H. Kil, S. J. Oh, D. Y. Chi, K. Kim, K. Choi, I. C. Kwon, S. Y. Kim, *J. Controlled Release* **2010**, *147*, 253 – 260; c) M. E. Fox, S. Guillaudeu, J. M. J. Frechet, K. Jerger, N. Macaraeg, F. C. Szoka, *Mol. Pharm.* **2009**, *6*, 1562 – 1572.

[11] a) V. Bala, S. S. Rao, B. J. Boyd, C. A. Prestidge, *J. Controlled Release* **2013**, *172*, 48 – 61; b) Z. Zhou, X. Ma, E. Jin, J. Tang, M. Sui, Y. Shen, E. A. Van Kirk, W. J. Murdoch, M. Radosz, *Biomaterials* **2013**, *34*, 5722 – 5735.

[12] M. J. Ratain, *J. Clin. Oncol.* **2002**, *20*, 7 – 8.

[13] a) Y. E. Kurtoglu, M. K. Mishra, S. Kannan, R. M. Kannan, *Int. J. Pharm.* **2010**, *384*, 189 – 194; b) Y. Zhong, L. Shao, Y. Li, *Int. J. Oncol.* **2013**, *42*, 373 – 383.

[14] a) X. Hu, J. Hu, J. Tian, Z. Ge, G. Zhang, K. Luo, S. Liu, *J. Am. Chem. Soc.* **2013**, *135*, 17617 – 17629; b) A. G. Cheetham, P. Zhang, Y. A. Lin, L. L. Lock, H. Cui, *J. Am. Chem. Soc.* **2013**, *135*, 2907 – 2910.

[15] a) Y. Zhang, Q. Yin, L. Yin, L. Ma, L. Tang, J. Cheng, *Angew. Chem. Int. Ed.* **2013**, *52*, 6435 – 6439; *Angew. Chem.* **2013**, *125*, 6563 – 6567; b) S. McRae Page, M. Martorella, S. Parelkar, I. Kosif, T. Emrick, *Mol. Pharm.* **2013**, *10*, 2684 – 2692.

[16] X. Liu, J. Zhang, L. Song, B. C. Lynn, T. G. Burke, *J. Pharm. Biomed. Anal.* **2004**, *35*, 1113 – 1125.

[17] G. Helmlinger, F. Yuan, M. Dellian, R. K. Jain, *Nat. Med.* **1997**, *3*, 177 – 182.

[18] Q. Sun, M. Radosz, Y. Shen, *J. Controlled Release* **2012**, *164*, 156 – 169.

[19] a) P. Xu, E. A. Van Kirk, Y. Zhan, W. J. Murdoch, M. Radosz, Y. Shen, *Angew. Chem. Int. Ed.* **2007**, *46*, 4999 – 5002; *Angew. Chem.* **2007**, *119*, 5087 – 5090; b) Y. Lee, T. Ishii, H. Cabral, H. J. Kim, J. H. Seo, N. Nishiyama, H. Oshima, K. Osada, K. Kataoka, *Angew. Chem. Int. Ed.* **2009**, *48*, 5309 – 5312; *Angew. Chem.* **2009**, *121*, 5413 – 5416; c) Z. Zhou, Y. Shen, J. Tang, M. Fan, E. A. Van Kirk, W. J. Murdoch, M. Radosz, *Adv. Funct. Mater.* **2009**, *19*, 3580 – 3589; d) J. Du, T. Sun, W. Song, J. Wu, J. Wang, *Angew. Chem. Int. Ed.* **2010**, *49*, 3621 – 3626; *Angew. Chem.* **2010**, *122*, 3703 – 3708; e) Z. Zhou, Y. Shen, J. Tang, E. Jin, X. Ma, Q. Sun, B. Zhang, E. A. Van Kirk, W. J. Murdoch, *J. Mater. Chem.* **2011**, *21*, 19114 – 19123.

[20] P. Xu, E. A. VanKirk, W. J. Murdoch, Y. Zhan, D. D. Isaak, M. Radosz, Y. Shen, *Biomacromolecules* **2006**, *7*, 829 – 835.

[21] Y. Gao, Y. Chen, X. Ji, X. He, Q. Yin, Z. Zhang, J. Shi, Y. Li, *ACS Nano* **2011**, *5*, 9788 – 9798.

[22] N. Malik, R. Wiwattanapatapee, R. Klopsch, K. Lorenz, H. Frey, J. W. Weener, E. W. Meijer, W. Paulus, R. Duncan, *J. Controlled Release* **2000**, *65*, 133 – 148.

[23] K. T. Al-Jamal, W. T. Al-Jamal, S. Akerman, J. E. Podesta, A. Yilmazer, J. A. Turton, A. Bianco, N. Vargesson, C. Kanthou, A. T. Florence, G. M. Tozer, K. Kostarelos, *Proc. Natl. Acad. Sci. USA* **2010**, *107*, 3966 – 3971.

[24] U. Prabhakar, H. Maeda, R. K. Jain, E. M. Sevick-Muraca, W. Zamboni, O. C. Farokhzad, S. T. Barry, A. Gabizon, P. Grodzinski, D. C. Blakey, *Cancer Res.* **2013**, *73*, 2412 – 2417.

[25] J. Wang, X. Sun, W. Mao, W. Sun, J. Tang, M. Sui, Y. Shen, Z. Gu, *Adv. Mater.* **2013**, *25*, 3670 – 3676.

